

# Hybrid mid-infrared optical parametric chirped-pulse amplification system with a broadband non-collinear quasi-phase-matched power amplifier

B. W. Mayer,<sup>1,\*</sup> C. R. Phillips,<sup>1,†</sup> L. Gallmann,<sup>1,2</sup> and U. Keller<sup>1</sup>

<sup>1</sup>Department of Physics, Institute for Quantum Electronics, ETH Zurich, 8093 Zurich, Switzerland

<sup>2</sup>Institute of Applied Physics, University of Bern, 3012 Bern, Switzerland

\*Corresponding author: [mayerb@phys.ethz.ch](mailto:mayerb@phys.ethz.ch)

<sup>†</sup>These authors contributed equally

We report a hybrid OPCPA system with the capability of generating broadband mid-infrared idler pulses from a non-collinear quasi-phase-matched power amplifier on the basis of periodically poled MgO:LiNbO<sub>3</sub>. It is seeded by the idler generated from a two-stage collinear pre-amplifier based on aperiodically poled MgO:LiNbO<sub>3</sub>. The amplification and pulse compression scheme we use does not require any angular dispersion to be introduced or compensated for on either the seed or the generated idler pulses. The mid-IR idler output has a bandwidth of 800 nm centered at 3.4  $\mu\text{m}$ . After compression, we obtain a pulse duration of 43.1 fs (FWHM; 41.4-fs transform limit) and a pulse energy of 17.2  $\mu\text{J}$  at a repetition rate of 50 kHz.

Light sources emitting in the mid-infrared (mid-IR) spectral range with its potential for the generation of high-harmonics (HHG) beyond the water window have gained great attention for performing time-resolved studies and spectroscopic investigations of the dynamics on molecular systems [1-4]. Furthermore, probing the wavelength-scaling behavior of strong-field processes, such as photoionization, more deeply into the tunneling regime is one of the main motivations for developing longer-wavelength driving fields [5,6]. Additionally, ultrafast and high peak-power mid-IR light sources have been used for a number of accelerator applications, such as enhancing the electron peak current in x-ray free-electron-lasers [7].

Primarily, the lack of laser gain crystals allowing the emission of few-cycle mid-IR light directly from high-power chirped-pulse amplifiers (CPAs) triggered the investigation and development of optical amplifiers exploiting nonlinear conversion schemes, such as optical parametric chirped-pulse amplification (OPCPA). Great efforts have been put into the investigation of phase-matching schemes in the mid-IR spectral range compatible with broadband parametric amplification and frequency conversion [8-10].

Prominent candidates with the capability to support large amplification bandwidths in the mid-IR are periodically poled MgO:LiNbO<sub>3</sub> (PPLN) and aperiodically poled MgO:LiNbO<sub>3</sub> (APPLN). PPLN and more recently APPLN have been used for the generation of few-cycle mid-IR pulses in collinear, quasi phase-matched (QPM) OPCPA schemes [8,11-13], and for broadband difference-frequency generation (DFG) [9,14].

In this Letter, we present a proof-of-principle OPCPA system by combining a collinear chirped QPM pre-amplifier and a quasi-phase- and group-velocity- (GV-) matched power amplifier. Since we use a unique combination of these two distinct amplification schemes within one system, we refer to it as a hybrid OPCPA system (see Fig. 1). This represents a promising technique to obtain phase-matching over a very broad bandwidth in

the mid-IR spectral range. In our final power amplifier, GV-matching is enabled via a non-collinear beam geometry, in combination with the corresponding QPM period to achieve phase-matching. A related phase-matching scheme, based on seeding an OPCPA with an angularly chirped signal seed around 1.5  $\mu\text{m}$ , was proposed theoretically for PPLN [15], but not demonstrated experimentally until now.

The collinear QPM pre-amplifiers of our hybrid OPCPA system are described in [12]. In particular, the collinear geometry of the APPLN-based pre-amplification scheme has low angular sensitivity and allows us to generate a broadband and angular-dispersion-free idler as seed for the final broadband non-collinear PPLN power amplifier shown in Fig. 1. This amplifier delivers idler pulses with a spectral bandwidth ranging from 3.0  $\mu\text{m}$  to 3.8  $\mu\text{m}$ , corresponding to an optical bandwidth of 21 THz.

Before describing the experiment in more detail, we first discuss the operating principles of the new system. In

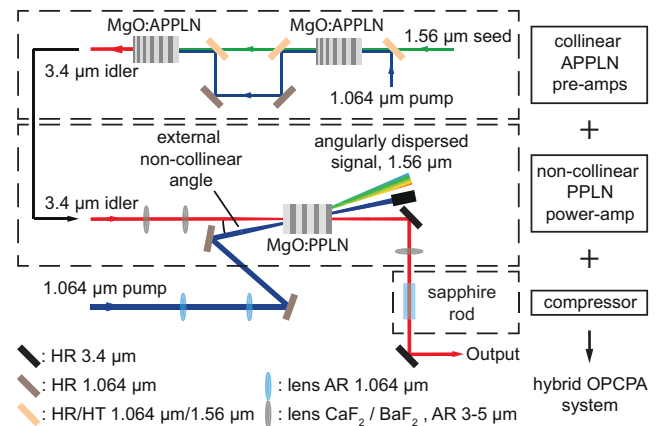


Fig. 1. Experimental setup of the mid-IR OPCPA. The two-stage, APPLN-based, collinear pre-amplifiers are shown in the upper half of the schematic. The angular-dispersion-free idler extracted from the pre-amplifier is used as seed for the non-collinear PPLN power amplifier shown in the lower half. AR: anti-reflective, HR: highly-reflective, HT: highly-transmissive.

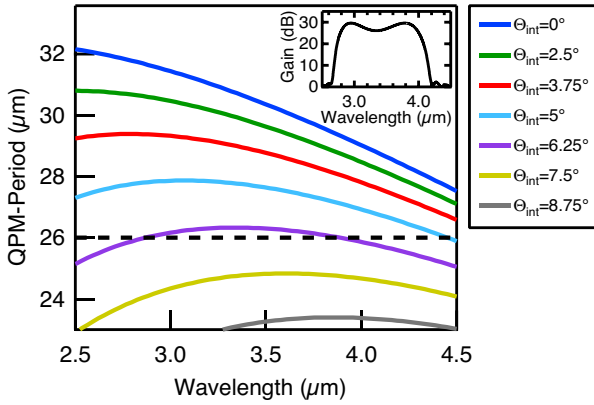


Fig. 2. Angular tunability of phase-matching for different non-collinear pump angles with respect to the idler seed. Introducing a non-collinear angle  $\Theta_{\text{int}}$  reduces the spread of  $\Delta k(\lambda)$  within a particular optical bandwidth. The black dashed line represents the QPM period used for the PPLN crystal. The inset shows an example small-signal gain spectrum for the present non-collinear phase-matching scheme.

PPLN OPA devices, the QPM period is chosen to achieve phase-matching around a particular center wavelength, with an associated spread of the material phase-mismatch  $\Delta k(\lambda)$ . The spectral range that can be amplified around this wavelength is then related to the spread of  $\Delta k(\lambda)$ , and to the coupling rate  $\gamma$  (in  $\text{m}^{-1}$ ) between the signal and idler fields. This coupling rate also determines the plane-wave small-signal power gain, according to the relation  $G = |\cosh(gL) + i\Delta k/(2g)\sinh(gL)|^2$ , where  $g = (\gamma^2 - (\Delta k/2)^2)^{1/2}$  and crystal length  $L$  [16]. A larger value of  $\gamma$  leads to increased bandwidth (gain over a wider range of  $\Delta k(\lambda)$ ), but  $\gamma$  is ultimately limited by the damage threshold since it scales linearly with the pump electric field. A complementary technique is to use a non-collinear arrangement, which can enable GV-matching to reduce the spread of  $\Delta k(\lambda)$  within a given optical bandwidth. The use of such a non-collinear arrangement alters the phase-matching conditions. In a QPM implementation, however, phase-matching can almost always be recovered by using a different QPM period, in contrast to conventional birefringent phase-matching.

To illustrate these features, in Fig. 2 we show the phase-matching curves for a mid-IR PPLN OPCA device, assuming mid-IR idler seeding collinear to the constant grating  $k$ -vector  $K_g$ , and a narrow-band non-collinear pump incident at an angle to the crystal  $c$ -axis (as depicted in Fig. 1). For each pump angle, a different range of QPM periods is required to perfectly phase-match a given optical bandwidth. In our experimental configuration, a turning point in this QPM period is located near  $3.4 \mu\text{m}$  when choosing an internal angle of  $\Theta_{\text{int}} \sim 6.25^\circ$  of the pump with respect to the idler inside the nonlinear crystal, and hence maximum bandwidth around this wavelength is achieved. The turning point in the QPM period corresponds to GV-matching between the signal and idler waves.

To understand the implications on broadband OPCA, the black curve of the inset in Fig. 2 shows an example gain spectrum made possible by such a device, assuming a coupling rate of  $\gamma = 2 \text{ mm}^{-1}$ . The QPM period in this

example is adjusted to yield a finite negative phase-mismatch at the GV-matching wavelength, leading to the dip in gain around  $3.4 \mu\text{m}$  [14], with the result that the wings of the spectrum experience higher parametric gain.

In our system (shown in Fig. 1), such a non-collinear PPLN stage serves as the power amplifier. It is seeded by the mid-IR idler output from an all-collinear two-stage OPCA based on APPLN; this part of the system consists of two weakly saturated amplifiers, from which the generated (unseeded)  $3.4\text{-}\mu\text{m}$  idler is extracted without the need to compensate for any angular chirp due to the collinear beam geometry. The APPLN OPCA itself is seeded by a mode-locked femtosecond fiber amplifier operating at  $\lambda = 1.56 \mu\text{m}$  and pumped by a  $1.064\text{-}\mu\text{m}$  industrial laser [12].

The generated idler seed pulses are temporally and spatially overlapped with the pump pulses in the power amplifier, which is pumped by a home-built Innoslab amplifier [17]. Based on our theoretical predictions we employ an internal pump angle of  $\sim 6.25^\circ$  with respect to the idler. The average powers for the seed and pump just before the uncoated 2-mm long, 2-mm by 2-mm wide PPLN crystal are 31 mW and 17.8 W, respectively. The pump is focused to an intensity of  $10.7 \text{ GW/cm}^2$  ( $1/e^2$ -radius of  $475 \mu\text{m}$  in the horizontal and  $350 \mu\text{m}$  in the vertical axis). In Fig. 3, we show the measured idler spectra before and after the power amplifier. There is evidence of increased parametric gain on the wings of the spectrum, which is consistent with the dip in the small-signal gain around the center wavelength shown in the inset of Fig. 2.

The amplified idler pulses were compressed by the careful design of sign and amount of dispersion of the near-IR seed pulses prior to the APPLN pre-amplifiers, in combination with bulk-propagation of the idler after the final power amplifier through an AR-coated, 50-mm-long sapphire rod. This method yielded a pulse duration shorter than four oscillation cycles of the electric field at the  $3.4 \mu\text{m}$  center wavelength [12]. Fig. 4 shows the measured and retrieved spectrograms, spectra and spectral phase from an SHG-FROG characterization. The residual fluctuation of the spectral phase results in a pedestal in the time domain. Note that, as discussed in [12], the fluctuations in spectral phase originate from our near-IR seeding scheme, rather than any of the OPCA devices. The reconstructed temporal intensity profile is shown in Fig. 4(d). The energy of the compressed idler pulse was  $17.2 \mu\text{J}$ , corresponding to an average power of

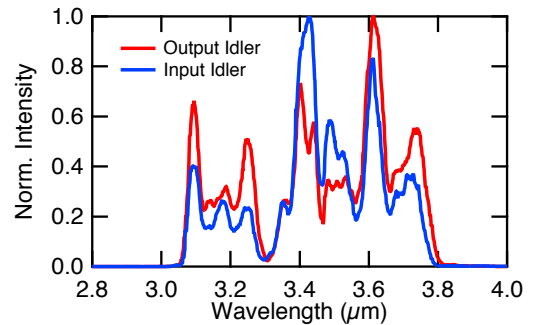


Fig. 3. Measured spectra of the input idler (blue) and output idler (red) of the non-collinear OPCA power amplifier.

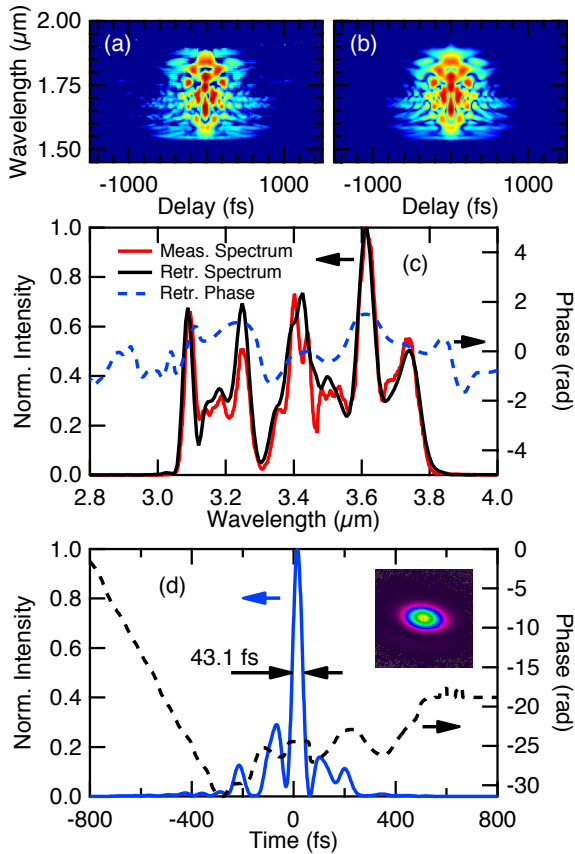


Fig. 4. (a): Measured SHG-FROG spectrogram. (b): Retrieved spectrogram. (c): Measured (red) and retrieved (black) idler spectrum and spectral phase (blue dashed) after compression. (d): Retrieved temporal intensity profile. The inset shows the idler beam profile. The FROG-error of the reconstruction for a grid size of 512 by 512 points is 0.0125.

0.86 W at the 50-kHz repetition-rate. We estimate an internal idler power (i.e. power inside the PPLN crystal) of 1.2 W (corresponding to 24  $\mu\text{J}$ ) when we account for all the linear losses encountered from the uncoated end-facets of the PPLN crystal and the optical elements arranged after the power amplifier. This power corresponds to an internal quantum conversion efficiency (number of idler photons at the end of the QPM grating divided by the number of pump photons at the input) of 25%. Thus, with coated crystals and the same input beam intensities, an idler energy of 24  $\mu\text{J}$  should be possible without changing any other aspects of the system.

To estimate the optical parametric generation (OPG) background, the signal seed was blocked before the first APPLN pre-amplifier. The spectrally resolved OPG background is shown in Fig. 5. We also measured its average power with a thermal power meter. The spectral characterization as well as the power measurements are within the noise floor of the respective detectors, indicating a negligible OPG background compared to the amplified pulses (<300  $\mu\text{W}$ ). Furthermore, we note that no evidence for photorefractive effects was observed.

The inset of Fig. 4(d) shows the beam profile of the compressed mid-IR idler. The fairly large non-collinear angle between the idler, signal and pump beams leads to some spatial walk-off within the crystal. This effect,

combined with the slight ellipticity of our pump beam, results in a slight ellipticity of the idler beam. The spatial walk-off effect imposes a constraint on the peak power of the pump that is needed to obtain a high parametric gain. For a characteristic non-collinear angle  $\theta$ , the ratio of transverse spatial walk-off  $w_{wo}$  to pump beam radius  $w_p$  can be expressed as  $w_{wo}/w_p = (\gamma L) \cdot \tan(\theta) / (\gamma w_p)$ . In this equation, the value of  $\theta$  is determined by the GV-matching condition; the  $(\gamma L)$  factor determines the small-signal OPA gain [16]; and, for a given nonlinear crystal,  $(\gamma w_p)^2$  is proportional to the peak power of the pump. For the configuration we use, assuming  $\theta = 6.25^\circ$  and a 50% QPM duty cycle with  $d_{33} = 19.5 \text{ pm/V}$  [18], a peak power of 14 MW is required to achieve a plane-wave small-signal gain of 30-dB while keeping  $w_{wo}/w_p < 0.5$ . The peak pump power we use is 24.1 MW, satisfying this constraint.

It is interesting to note that the amplification technique we have demonstrated is applicable to other QPM media as well, for example it could support broadband OPA in orientation-patterned GaAs (OP-GaAs) [19], with the potential for extending OPA and OPCPA into the far-IR spectral region [20]. To compare OP-GaAs to MgO:PPLN, note that our 1.064- $\mu\text{m}$  pump wavelength is somewhat longer than half the zero-dispersion wavelength (which is around 1.9  $\mu\text{m}$  in MgO:PPLN). An analogous configuration for OPA in OP-GaAs, whose zero-dispersion wavelength is around 6.6  $\mu\text{m}$  [21], would be to use a pump wavelength of  $\sim 3.4 \mu\text{m}$  or longer. This pumping configuration could support GV-matched OPCPA for center seed wavelengths from 7 to  $\sim 18 \mu\text{m}$ . Alternatively, using 2- $\mu\text{m}$  or 2.5- $\mu\text{m}$  pump lasers, GV-matching could be achieved for signal-seeded OP-GaAs devices. Therefore, the technique we have demonstrated may prove to be important in developing widely tunable and few-cycle sources in the far-IR as well as the mid-IR.

In conclusion we have demonstrated a proof-of-principle broadband mid-IR hybrid OPCPA system based on APPLN pre-amplification and a new non-collinear group-velocity-matched PPLN power amplifier. The idler seed pulses, centered around 3.4  $\mu\text{m}$ , are generated from two weakly-saturated all-collinear APPLN pre-amplifiers. These seed pulses are amplified to 17.2- $\mu\text{J}$  (energy measured after pulse compression), corresponding to an internal conversion efficiency of 25%. The pulses are compressed to 43.1 fs (corresponding to less than four

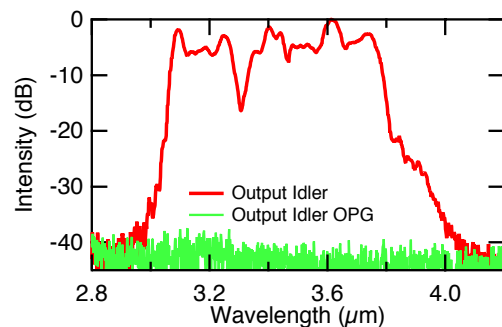


Fig. 5. Spectral characterization of the OPG background, measured by blocking the near-IR seed pulses before the first APPLN pre-amplifier, in comparison to the idler pulse spectrum. Our measurements show that the energy of this OPG background is at least 34.6 dB lower than the idler pulse energy.

optical cycles) by propagation through a bulk sapphire rod. Fine-tuning of the idler chirp is easily obtained by adjusting the pre-chirping of the 1.56- $\mu\text{m}$  signal seed before the pre-amplifiers. The efficiency of the beam-collimation and compression is  $>93\%$ . A clear step for future work is to use a pump with higher peak power, in order to mitigate spatial walk-off effects. Furthermore, the combination of GV-matched QPM demonstrated here and chirped QPM demonstrated previously [11,12] could enable even broader bandwidths, as well as customized gain profiles, by spatially varying the grating  $k$ -vector over the required range [22-25]. This approach, together with further power scaling achievable by the use of wide-aperture QPM devices as the gain medium [26] will have advantageous implications on the generation of energetic few-cycle mid-IR pulses to enable experimental studies of electron dynamics in atoms and molecules in attosecond and strong-field science.

This research was supported by the Swiss National Science Foundation (SNSF) through grant #200020\_144365/1, and by a Marie Curie International Incoming Fellowship within the 7th European Community Framework Programme.

## References

1. F. Krausz and M. Ivanov, *Rev. Mod. Phys.* **81**, 163 (2009).
2. M. C. Chen, P. Arpin, T. Popmintchev, M. Gerrity, B. Zhang, M. Seaberg, D. Popmintchev, M. M. Murnane, and H. C. Kapteyn, *Phys. Rev. Lett.* **105**, 173901 (2010).
3. T. Popmintchev, M.-C. Chen, D. Popmintchev, P. Arpin, S. Brown, S. Ališauskas, G. Andriukaitis, T. Balčiūnas, O. D. Mücke, A. Pugzlys, A. Baltuška, B. Shim, S. E. Schrauth, A. Gaeta, C. Hernández-García, L. Plaja, A. Becker, A. Jaron-Becker, M. M. Murnane, and H. C. Kapteyn, *Science* **336**, 1287 (2012).
4. P. Hamm, M. Zurek, W. Mäntele, M. Meyer, H. Scheer, and W. Zinth, *Proc. Natl. Acad. Sci. U.S.A.* **92**, 1826 (1995).
5. P. Colosimo, G. Doumy, C. I. Blaga, J. Wheeler, C. Hauri, F. Catoire, J. Tate, R. Chirla, A. M. March, G. G. Paulus, H. G. Muller, P. Agostini, and L. F. DiMauro, *Nat. Phys.* **4**, 386 (2008).
6. D. D. Hickstein, P. Ranitovic, S. Witte, X.-M. Tong, Y. Huismans, P. Arpin, X. Zhou, K. E. Keister, C. W. Hogle, B. Zhang, C. Ding, P. Johnsson, N. Toshima, M. J. J. Vrakking, M. M. Murnane, and H. C. Kapteyn, *Phys. Rev. Lett.* **109**, 073004 (2012).
7. A. A. Zholents, *Phys. Rev. Spec. Top.-Acc. Beams* **8**, 040701 (2005).
8. C. Heese, C. R. Phillips, L. Gallmann, M. M. Fejer, and U. Keller, *Opt. Lett.* **35**, 2340 (2010).
9. H. Suchowski, P. R. Krogen, S.-W. Huang, F. X. Kärtner, and J. Moses, *Opt. Express* **21**, 28892 (2013).
10. H. Fattahi, A. Schwarz, S. Keiber, and N. Karpowicz, *Opt. Lett.* **38**, 4216 (2013).
11. C. Heese, C. R. Phillips, B. W. Mayer, L. Gallmann, M. M. Fejer, and U. Keller, *Opt. Express* **20**, 26888 (2012).
12. B. W. Mayer, C. R. Phillips, L. Gallmann, M. M. Fejer, and U. Keller, *Opt. Lett.* **38**, 4265 (2013).
13. M. Hemmer, A. Thai, M. Baudisch, H. Ishizuki, T. Taira, and J. Biegert, *Chin. Opt. Lett.* **11**, 013202 (2013).
14. Y. Deng, A. Schwarz, H. Fattahi, M. Ueffing, X. Gu, M. Ossiander, T. Metzger, V. Pervak, H. Ishizuki, T. Taira, T. Kobayashi, G. Marcus, F. Krausz, R. Kienberger, and N. Karpowicz, *Opt. Lett.* **37**, 4973 (2012).
15. S.-W. Huang, J. Moses, and F. X. Kärtner, *Opt. Lett.* **37**, 2796 (2012).
16. R. A. Baumgartner and R. Byer, *IEEE J. Quant. Elect.* **15**, 432 (1979).
17. C. Heese, A. E. Oehler, L. Gallmann, and U. Keller, *Appl. Phys. B* **103**, 5 (2011).
18. I. Shoji, T. Kondo, A. Kitamoto, M. Shirane, and R. Ito, *J. Opt. Soc. Am. B* **14**, 2268 (1997).
19. L. A. Eyres, P. J. Tourreau, T. J. Pinguet, C. B. Ebert, J. S. Harris, M. M. Fejer, L. Becouarn, B. Gerard, and E. Lallier, *Appl. Phys. Lett.* **79**, 904 (2001).
20. C. R. Phillips, J. Jiang, C. Mohr, A. C. Lin, C. Langrock, M. Snure, D. Bliss, M. Zhu, I. Hartl, J. S. Harris, M. E. Fermann, and M. M. Fejer, *Opt. Lett.* **37**, 2928 (2012).
21. P. S. Kuo, K. L. Vodopyanov, M. M. Fejer, D. M. Simanovskii, X. Yu, J. S. Harris, D. Bliss, and D. Weyburne, *Opt. Lett.* **31**, 71 (2006).
22. M. Charbonneau-Lefort, B. Afeyan, and M. M. Fejer, *J. Opt. Soc. Am. B* **25**, 463 (2008).
23. C. R. Phillips, C. Langrock, D. Chang, Y. W. Lin, L. Gallmann, and M. M. Fejer, *J. Opt. Soc. Am. B* **30**, 1551 (2013).
24. C. R. Phillips, L. Gallmann, and M. M. Fejer, *Opt. Express* **21**, 10139 (2013).
25. C. R. Phillips, B. W. Mayer, L. Gallmann, M. M. Fejer, and U. Keller, *Opt. Express.*, (submitted).
26. H. Ishizuki and T. Taira, *Opt. Express* **20**, 20002 (2012).

- [1] F. Krausz and M. Ivanov, "Attosecond physics," *Rev. Mod. Phys.* **81**, 163 (2009).
- [2] M. C. Chen, P. Arpin, T. Popmintchev, M. Gerrity, B. Zhang, M. Seaberg, D. Popmintchev, M. M. Murnane, and H. C. Kapteyn, "Bright, Coherent, Ultrafast Soft X-Ray Harmonics Spanning the Water Window from a Tabletop Light Source," *Physical Review Letters* **105**, 173901 (2010).
- [3] T. Popmintchev, M.-C. Chen, D. Popmintchev, P. Arpin, S. Brown, S. Ališauskas, G. Andriukaitis, T. Balčiunas, O. D. Mücke, A. Pugzlys, A. Baltuška, B. Shim, S. E. Schrauth, A. Gaeta, C. Hernández-García, L. Plaja, A. Becker, A. Jaron-Becker, M. M. Murnane, and H. C. Kapteyn, "Bright Coherent Ultrahigh Harmonics in the keV X-ray Regime from Mid-Infrared Femtosecond Lasers," *Science* **336**, 1287-1291 (2012).
- [4] P. Hamm, M. Zurek, W. Mäntele, M. Meyer, H. Scheer, and W. Zinth, "Femtosecond infrared spectroscopy of reaction centers from Rhodobacter sphaeroides between 1000 and 1800  $\text{cm}^{-1}$ ," *Proc. Natl. Acad. Sci. U.S.A.* **92**, 1826-1830 (1995).
- [5] P. Colosimo, G. Doumy, C. I. Blaga, J. Wheeler, C. Hauri, F. Catoire, J. Tate, R. Chirla, A. M. March, G. G. Paulus, H. G. Muller, P. Agostini, and L. F. DiMauro, "Scaling strong-field interactions towards the classical limit," *Nature Physics* **4**, 386-389 (2008).
- [6] D. D. Hickstein, P. Ranitovic, S. Witte, X.-M. Tong, Y. Huismans, P. Arpin, X. Zhou, K. E. Keister, C. W. Hogle, B. Zhang, C. Ding, P. Johnsson, N. Tushima, M. J. J. Vrakking, M. M. Murnane, and H. C. Kapteyn, "Direct Visualization of Laser-Driven Electron Multiple Scattering and Tunneling Distance in Strong-Field Ionization," *Physical Review Letters* **109**, 073004 (2012).
- [7] A. A. Zholents, "Method of an enhanced self-amplified spontaneous emission for x-ray free electron lasers," *Physical Review Special Topics - Accelerators and Beams* **8**, 040701 (2005).
- [8] C. Heese, C. R. Phillips, L. Gallmann, M. M. Fejer, and U. Keller, "Ultrabroadband, highly flexible amplifier for ultrashort midinfrared laser pulses based on aperiodically poled  $\text{Mg}:\text{LiNbO}_3$ ," *Opt. Lett.* **35**, 2340-2342 (2010).
- [9] H. Suchowski, P. R. Krogen, S.-W. Huang, F. X. Kärtner, and J. Moses, "Octave-spanning coherent mid-IR generation via adiabatic difference frequency conversion," *Opt. Express* **21**, 28892-28901 (2013).
- [10] H. Fattahi, A. Schwarz, S. Keiber, and N. Karpowicz, "Efficient, octave-spanning difference-frequency generation using few-cycle pulses in simple collinear geometry," *Optics Letters* **38**, 4216-4219 (2013).
- [11] C. Heese, C. R. Phillips, B. W. Mayer, L. Gallmann, M. M. Fejer, and U. Keller, "75 MW few-cycle mid-infrared pulses from a collinear apodized APPLN-based OPCPA," *Opt. Express* **20**, 26888 (2012).
- [12] B. W. Mayer, C. R. Phillips, L. Gallmann, M. M. Fejer, and U. Keller, "Sub-four-cycle laser pulses directly from a high-repetition-rate optical parametric chirped-pulse amplifier at 3.4  $\mu\text{m}$ ," *Opt. Lett.* **38**, 4265-4268 (2013).
- [13] M. Hemmer, A. Thai, M. Baudisch, H. Ishizuki, T. Taira, and J. Biegert, "18  $\mu\text{J}$  energy, 160-kHz repetition rate, 250-MW peak power mid-IR OPCPA," *Chin. Opt. Lett.* **11**, 013202 (2013).
- [14] Y. Deng, A. Schwarz, H. Fattahi, M. Ueffing, X. Gu, M. Ossiander, T. Metzger, V. Pervak, H. Ishizuki, T. Taira, T. Kobayashi, G. Marcus, F. Krausz, R. Kienberger, and N. Karpowicz, "Carrier-envelope-phase-stable, 1.2 mJ, 1.5 cycle laser pulses at 2.1  $\mu\text{m}$ ," *Opt. Lett.* **37**, 4973-4975 (2012).
- [15] S.-W. Huang, J. Moses, and F. X. Kärtner, "Broadband noncollinear optical parametric amplification without angularly dispersed idler," *Opt. Lett.* **37**, 2796-2798 (2012).
- [16] R. A. Baumgartner and R. Byer, "Optical parametric amplification," *IEEE Journal of Quantum Electronics* **15**, 432-444 (1979).
- [17] C. Heese, A. E. Oehler, L. Gallmann, and U. Keller, "High-energy picosecond  $\text{Nd}:\text{YVO}_4$  slab amplifier for OPCPA pumping," *Appl. Phys. B* **103**, 5-8 (2011).
- [18] I. Shoji, T. Kondo, A. Kitamoto, M. Shirane, and R. Ito, "Absolute scale of second-order nonlinear-optical coefficients," *J. Opt. Soc. Am. B* **14**, 2268-2294 (1997).
- [19] L. A. Eyres, P. J. Tourreau, T. J. Pinguet, C. B. Ebert, J. S. Harris, M. M. Fejer, L. Becouarn, B. Gerard, and E. Lallier, "All-epitaxial fabrication of thick, orientation-patterned GaAs films for nonlinear optical frequency conversion," *Appl. Phys. Lett.* **79**, 904-906 (2001).
- [20] C. R. Phillips, J. Jiang, C. Mohr, A. C. Lin, C. Langrock, M. Snure, D. Bliss, M. Zhu, I. Hartl, J. S. Harris, M. E. Fermann, and M. M. Fejer, "Widely tunable midinfrared difference frequency generation in orientation-patterned GaAs pumped with a femtosecond Tm-fiber system," *Optics Letters* **37**, 2928-2930 (2012).
- [21] P. S. Kuo, K. L. Vodopyanov, M. M. Fejer, D. M. Simanovskii, X. Yu, J. S. Harris, D. Bliss, and D. Weyburne, "Optical parametric generation of a mid-infrared continuum in orientation-patterned GaAs," *Optics Letters* **31**, 71-73 (2006).
- [22] M. Charbonneau-Lefort, B. Afeyan, and M. M. Fejer, "Optical parametric amplifiers using chirped quasi-phase-matching gratings I: practical design formulas," *J. Opt. Soc. Am. B* **25**, 463-480 (2008).
- [23] C. R. Phillips, C. Langrock, D. Chang, Y. W. Lin, L. Gallmann, and M. M. Fejer, "Apodization of chirped quasi-phaseshifting devices," *J. Opt. Soc. Am. B* **30**, 1551-1568 (2013).
- [24] C. R. Phillips, L. Gallmann, and M. M. Fejer, "Design of quasi-phase-matching gratings via convex optimization," *Optics Express* **21**, 10139-10159 (2013).
- [25] C. R. Phillips, B. W. Mayer, L. Gallmann, M. M. Fejer, and U. Keller, "Design constraints of optical parametric chirped pulse amplification based on chirped quasi-phase-matching gratings," *Optics Express*, (submitted).
- [26] H. Ishizuki and T. Taira, "Half-joule output optical-parametric oscillation by using 10-mm-thick periodically poled Mg-doped congruent  $\text{LiNbO}_3$ ," *Optics Express* **20**, 20002-20010 (2012).